1997 HST Calibration Workshop
Space Telescope Science Institute, 1997
S. Casertano, et al., eds.

STIS First-Order Low-Resolution Mode Point-Source Sensitivity Curves

Nicholas Collins

Hughes STX/LASP/GSFC

Ralph Bohlin

Space Telescope Science Institute, 3700 San Martin Drive, Baltimore, MD 21218

Abstract. Point source sensitivity curves have been derived for the first order modes G140L ($\lambda_{central}$ =1425Å), G230L (2376Å), G230LB (2375Å), G430L (4300Å), and G750L (7751Å), spanning a wavelength range from 1140Å to 10320Å. The curves are determined by comparing wide slit ($52'' \times 2''$) observations of the spectrophotometric standard star GD 153 to a pure hydrogen white dwarf model (Bohlin 1996). The calibration is tested by applying the curves to a STIS observation of the spectrophotometric standard star BD+75D325, and comparing these flux calibrated observations to a calibrated FOS spectrum.

1. Introduction

A sensitivity curve is used to determine the flux of an observed point-source spectrum by

$$f_{obs} = C_{obs}/S \tag{1}$$

where f_{obs} is the calibrated spectrum, C_{obs} is the observed spectrum in counts $\cdot$ pixel^{-1} $\cdot$ second^{-1}, and S is the sensitivity as a function of wavelength. The sensitivity is derived by

$$S = C_{std}/f_{std} \tag{2}$$

where C_{std} is an observation of a spectrophotometric standard star in counts $\cdot$ pixel^{-1} $\cdot$ second^{-1}, and f_{std} is a calibrated spectrum of the same standard from some other source, or a model of the standard spectrum.

The "pixel^{-1}" in the units for C refers to the cross-dispersion direction, and arises from the extraction of a point source spectrum on a two-dimensional detector using a fixed extraction height.

2. The Data Set

Observations of the pure hydrogen white dwarf GD 153 (Bohlin, Colina, & Finley 1995) are used to define the sensitivity curve, since these data are the only set of observations of a fundamental standard in all five low-resolution spectral modes. GD 153 is a preferred calibration standard, because the only lines are from HI and because Bohlin (1996) defined the FOS calibration with a set of four pure hydrogen WD models that includes GD 153. An input spectrum with many lines might produce a confusing sensitivity curve, if the model (or reference) line profiles do not perfectly match those of the observed spectrum.

2.1. Observations

All input spectra were obtained using the clear aperture # 38 ($52'' \times 2''$).

Two averaged observations comprise the input spectrum for the far-UV MAMA mode G140L. Only one near-UV (G230L) observation of GD 153 was obtained through aperture # 38. For each of the three CCD modes (G230LB, G430L, and G750L), seven observations were averaged to produce high signal to noise spectra. The component spectra that make up the average spectrum for each mode are listed in Table 1.

Table 1. Observations

Rootname	Observation Date	Target	Optical Element	CRSPLIT	Total ExpTime (sec.)	Slit Number	Slit Size (")
O43J01QAM	09/07/97	GD153	G140L	0	60.0	38	52x2
O3ZX08HHM	13/07/97	GD153	G140L	0	187.0	38	52x2
O3ZX08HLM	13/07/97	GD153	G230L	0	187.1	38	52x2
O3TT42010	21/05/97	GD153	G230LB	2	600.0	38	52x2
O3TT43010	28/05/97	GD153	G230LB	2	600.0	38	52x2
O3TT44010	04/06/97	GD153	G230LB	2	600.0	38	52x2
O3TT45010	10/06/97	GD153	G230LB	2	600.0	38	52x2
O3TT46010	18/06/97	GD153	G230LB	2	600.0	38	52x2
O3TT47010	25/06/97	GD153	G230LB	2	600.0	38	52x2
O3TT48010	01/07/97	GD153	G230LB	2	600.0	38	52x2
O3TT42020	21/05/97	GD153	G430L	2	252.0	38	52x2
O3TT43020	28/05/97	GD153	G430L	2	252.0	38	52x2
O3TT44020	04/06/97	GD153	G430L	2	252.0	38	52x2
O3TT45020	10/06/97	GD153	G430L	2	252.0	38	52x2
O3TT46020	18/06/97	GD153	G430L	2	252.0	38	52x2
O3TT47020	25/06/97	GD153	G430L	2	252.0	38	52x2
O3TT48020	01/07/97	GD153	G430L	2	252.0	38	52x2
O3TT42040	21/05/97	GD153	G750L	2	3240.0	38	52x2
O3TT43040	28/05/97	GD153	G750L	2	3240.0	38	52x2
O3TT44040	04/06/97	GD153	G750L	2	3240.0	38	52x2
O3TT45040	10/06/97	GD153	G750L	2	3240.0	38	52x2
O3TT46040	18/06/97	GD153	G750L	2	2282.0	38	52x2
O3TT47040	25/06/97	GD153	G750L	2	2282.0	38	52x2
O3TT48040	01/07/97	GD153	G750L	2	2282.0	38	52x2

The spectral extraction heights for the component spectra are 11 pixels for G140L and G230L, and 7 pixels for G230LB, G430L, and G750L (Leitherer & Bohlin 1997).

Each of the seven component G750L spectra was fringe-corrected at long wavelengths using a library tungsten lamp flat before averaging them together. For this data set, all tungsten lamp flats used were obtained through slit # 35 ($52'' \times 0''.1$). Briefly, the library flats are generated by (Plait, 1997)

- removing the lamp spectrum from the flat,
- removing scattered light (as determined by profiles obtained along the fiducial bars in the dispersion direction),

Profiles of the data and library flat are cross-correlated to ensure that the fringes in both are in phase. If the fringes are not in phase, the library flat is shifted (typically less than 1 pixel) to match the phase of the fringes in the data. The shifted library flat is then applied to the data image.

2.2. Reference Spectrum

The reference spectrum, GD153_MOD_002, is a pure hydrogen white dwarf model normalized to Landolt's visual photometry (Bohlin 1996). The spectrum was obtained from the

Calibration Data Base System (CDBS) at `http://www.stsci.edu/ftp/instrument/news/Observatory/astronomical_catalogs.html`.

3. Data Reduction

For each optical mode, the reference spectrum is integrated to match the resolution of each co-added observation, then divided into the observed spectrum, yielding a sensitivity curve in units of

$$\frac{counts \cdot pixel^{-1} \cdot second^{-1}}{ergs \cdot second^{-1} \cdot cm^{-2} \cdot \mathring{A}^{-1}}$$

A spline fit with evenly spaced nodes is performed to each raw curve in order to obtain a smooth sensitivity curve. Each fit is refined by interactively selecting more nodes in regions where a curve varies greatly with small changes in wavelength. Table 2 lists the number of nodes used within the nominal wavelength range for each mode. The wavelength region 1200Å - 1225Å in mode G140L is masked to exclude the strong Lyα feature from the fit. Small residuals at the Balmer lines on G430L and G750L are caused by slight differences in resolution between STIS and the model spectrum.

Some of the sensitivity curve spline fits are extrapolated at either end by at most 20 pixels to account for future planned spectral format, or MSM, shifts. No extrapolation is done past very low signal-to-noise regions. Some curves are cut off in low signal-to-noise regions. Table 2 lists the extrapolated and cropped regions for each mode.

Table 2. Sensitivity Curve Extrapolation Regions

Optical Element	Spline Nodes	Nominal Range(Å)	Short-λ Extrap.(Å)	Long-λ Extrap.(Å)	Short-λ Cutoff (Å)	Full Range (Å)
G140L	26	1118 - 1713	no extrap.	1713 - 1724	1140Å	1140 - 1724
G230L	28	1563 - 3140	no extrap.	3140 - 3171	1600Å	1600 - 3171
G230LB	28	1664 - 3066	1650 - 1664	3066 - 3093	-	1650 - 3093
G430L	40	2885 - 5691	2881 - 2884	5691 - 5746	-	2881 - 5746
G750L	42	5235 - 10229	no extrap.	10229 - 10327	-	5235 - 10327

4. Results

The sensitivity curves and their residuals are shown in Figures 1–5. The spline fit and extrapolations described above are represented by the dashed line in each plot. The spline nodes are plotted with diamonds.

4.1. Error Analysis

The residuals shown in Figures 1–5 are determined by dividing each curve by its spline fit, and are plotted for the wavelength ranges listed in Table 3. Table 3 lists the percent root-mean-squared residuals averaged over all wavelengths for each mode. Average RMS residuals are listed for three wavelength ranges for mode G750L to show how the scatter increases in the long wavelength region subject to fringing.

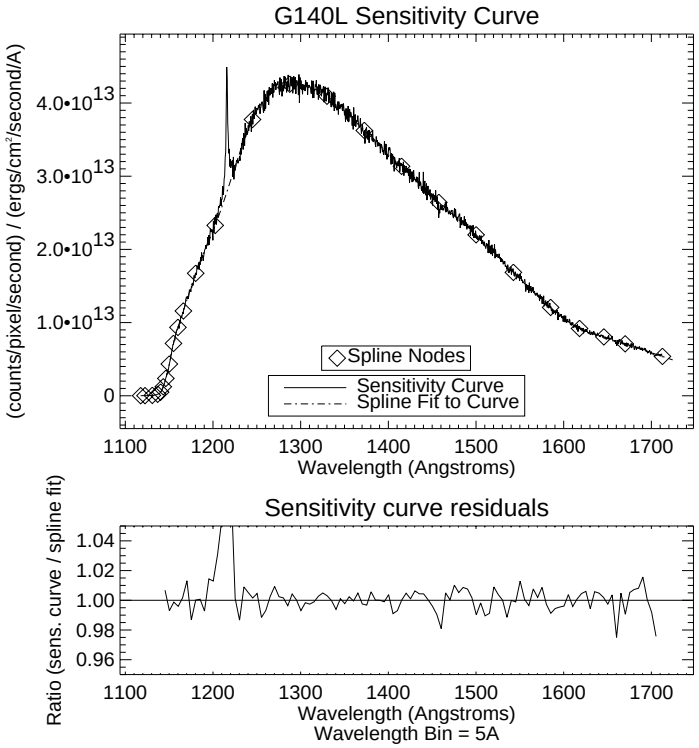

Figure 1. Sensitivity curve for optical element G140L, derived from 2 averaged observations of GD 153.

Table 3. Average Percent RMS Deviation for Each Mode

Optical Element	Wavelength Range(Å)	Avg. $\%\sigma_{rms}$
G140L[a]	1140-1200 and 1225-1713	1.35
G230L	1600 - 3140	1.35
G230LB	1664 - 3066	0.47
G430L	2885 - 5691	0.94
G750L	5235 - 8000	0.57
G750L	8000 - 9000	0.86
G750L	9000 - 10229	1.95

[a]Residuals in the region of the strong Lyα feature (1220-1225Å) are not included in the computation of σ_{rms}.

There is currently no flat field for the G140L mode, which makes the derived sensitivity subject to larger uncertainty at non-standard positions on the detector. For the other modes, the uncertainty in the calibration for continuum fluxes is estimated at ∼3% from a ∼2% uncertainty in the model absolute flux (Bohlin, Colina and Finley 1995) and from the 1-2% photometric repeatability of STIS spectra, as long as the spectra hit the same position on the detector to approximately one pixel. Scattered light from the instrumental PSF fills in the line profile at Lyman-alpha by ∼10% of the continuum level in comparison to the model line profile, as confirmed by FOS observations.

An estimation of the photometric uncertainty in the extrapolated regions is made by computing the average RMS residuals near the extrapolated region and is listed in Table 4. Column (1) lists the optical mode, column (2) lists the wavelength range near the

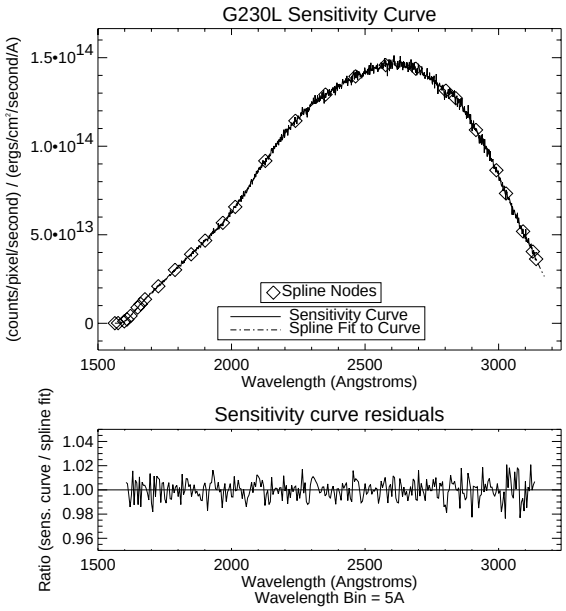

Figure 2. G230L Sensitivity Curve

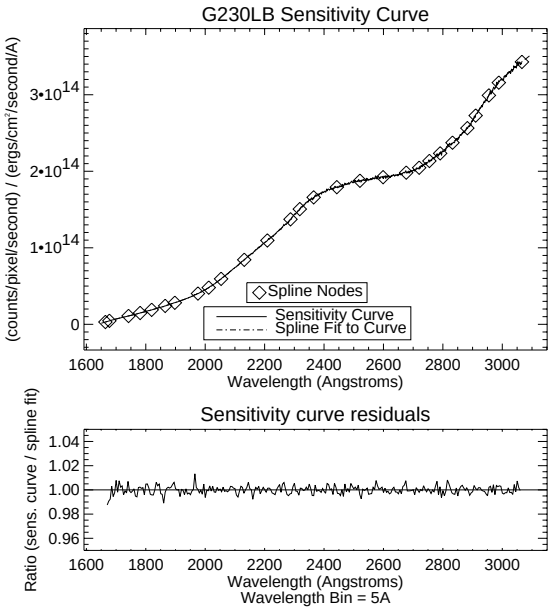

Figure 3. G230LB Sensitivity Curve

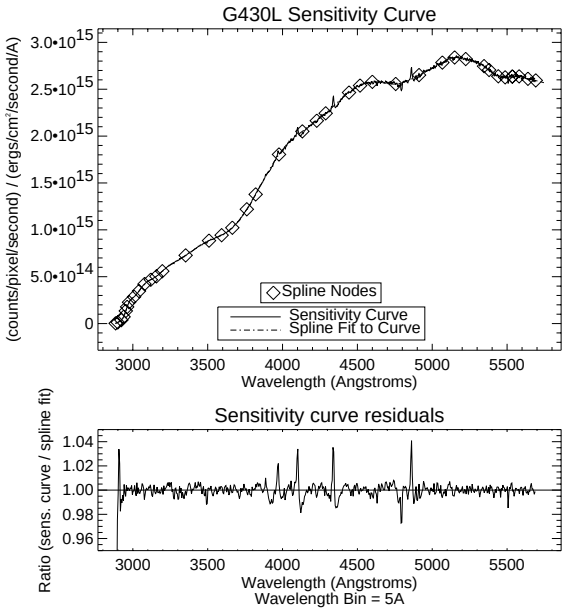

Figure 4. G430L Sensitivity Curve

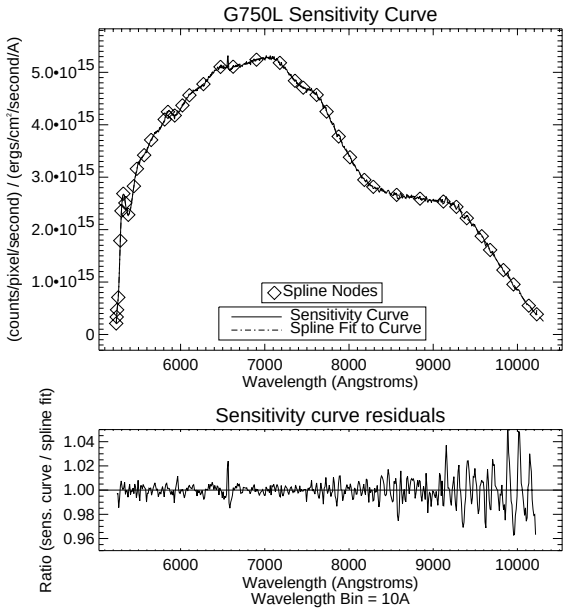

Figure 5. G750L Sensitivity Curve

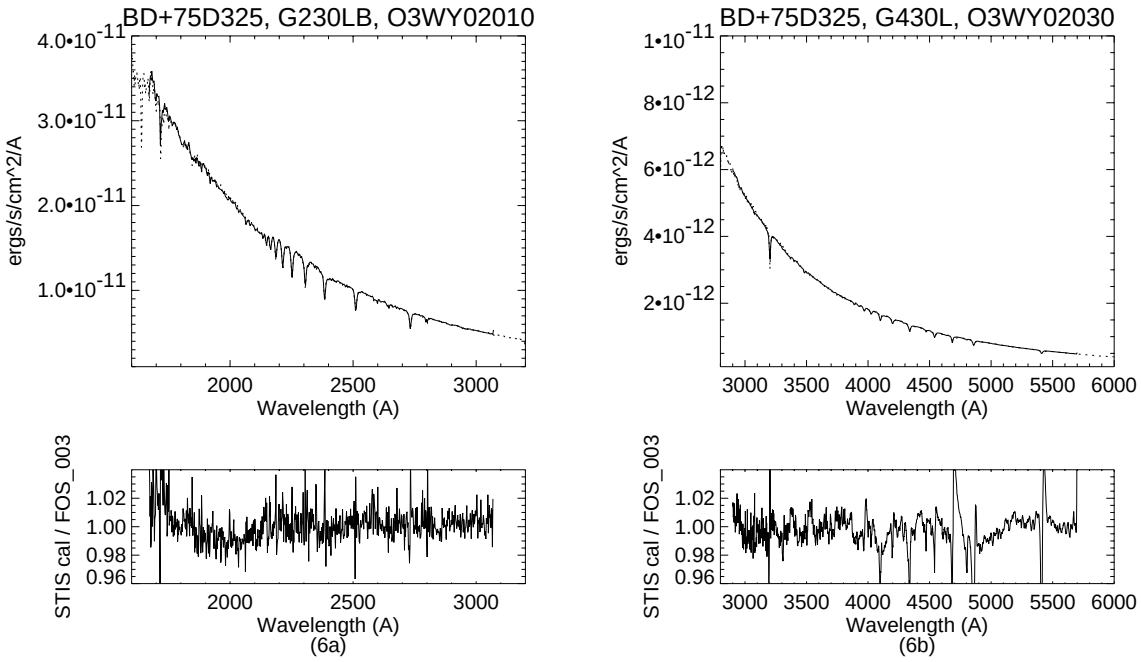

Figure 6. Sensitivity curves for G230LB (left panel) and G430L (right panel) applied to observations of BD+75D325. Top plot: calibrated STIS observation (solid line), and reference spectrum BD_75D325_FOS_003 (Bohlin 1996) (dotted line). Bottom plot: ratio of calibrated STIS spectrum to FOS spectrum.

extrapolation for that mode, and column (3) lists the average RMS percent uncertainty in that range.

Table 4. Estimated Average Percent RMS Deviation for Extrapolated Regions

Optical Element	Wavelength Range(Å)	Est. Avg. $\%\sigma_{rms}$
G140L	1700 - 1713	2.30
G230L	3110 - 3140	2.20
G230LB	1664 - 1678	0.85
G230LB	3033 - 3066	0.49
G430L	2884 - 2890	4.30
G430L	5640 -5690	0.37
G750L	10100 - 10200	1.97

4.2. A Test Case: Application of the Sensitivity Curves to Observations of BD+75D325

The left and right panels of Figure show STIS observations of BD+75D325 calibrated with the sensitivity curves described in this paper and plotted over an FOS spectrum (Bohlin 1996) of the same star. The FOS spectrum, BD+75D325, is obtained from the CDBS at the URL listed in section 2.2. The residuals plotted in the figures are the ratio of the calibrated STIS observation (integrated to the wavelength scale of the FOS spectrum) to the FOS spectrum. Average percent RMS uncertainties are 1.33% and 1.52% for G230LB and G430L, respectively. These values are consistent with the combined uncertainties of

the STIS calibration (see Table 3) and of the photometric accuracy of the FOS spectrum (1-2%) (Bohlin 1996).

Acknowledgments. We wish to thank Don Lindler and Phil Plait for essential data reduction advice.

References

Bohlin, R. C. 1996, AJ, 111, 1743

Bohlin, R. C., Colina, L., & Finley, D. S. 1995, AJ, 110, 1316.

Leitherer, C. & Bohlin, R., 1997, Instrument Science Report STIS 97-13 (Baltimore:STScI)

Plait, P. 1997, this volume